ACS Catalysis

pubs.acs.org/acscatalysis

Research Article

Dual-Chain Polymerization at an Early Transition-Metal Single-Site Catalyst

Tanner McDaniel,[†] Nicholas E. Smith,[†] Eric Cueny, and Clark R. Landis*

Cite This: *ACS Catal.* 2022, 12, 10680−10689

Read Online

ACCESS | Metrics & More | Article Recommendations | Supporting Information

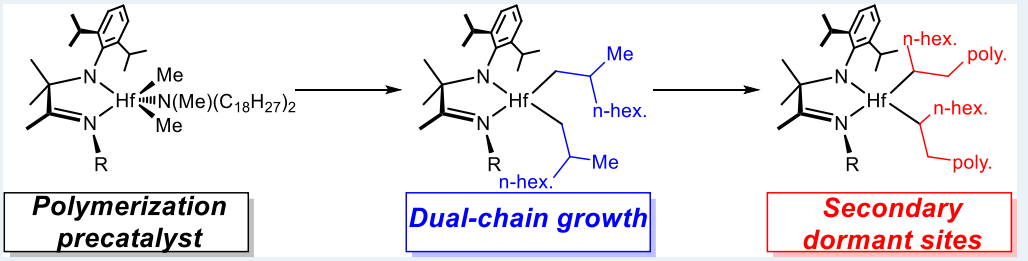

ABSTRACT: The hafnium complex $(N^{oct}N^{dipp})Hf(Me)_3$ (**1**, $N^{oct}N^{dipp}$ = *N*-octyl-*N*′-(2,6-diisopropylphenyl)-1,4-diaza-2,3,3-trimethyl-1-butene) contains a bidentate imino-anilido ligand. This complex undergoes protonolysis by the ammonium Brønsted acid $[HN(Me)(C_{18}H_{37})_2][B(C_6F_5)_4]$ to produce a competent alkene polymerization precatalyst, $[(N^{oct}N^{dipp})Hf(Me)_2(N(Me)(C_{18}H_{37})_2)][B(C_6F_5)_4]$ (**2**). Unlike most alkene polymerization precatalysts, **2** contains two Hf−Me groups, which have the potential to initiate and propagate two polymer chains simultaneously. Herein, we demonstrate that **2** does indeed grow two polymer chains at each hafnium center. Additional unusual characteristics for an early transition-metal catalyst include: (1) the number-average polymer molar mass (M_n) is independent of the concentration of monomer; (2) linear plots of monomer concentration as a function of time during polymerization indicate apparent zeroth-order dependence of rate on the monomer concentration; and (3) apparent first-order dependence of steady-state rate of polymerization on the *initial* concentration of monomer. While saturation behavior with respect to monomer concentration is common with late transition-metal-derived catalysts, propagation rate laws for early transition-metal complexes overwhelmingly are first-order in monomer concentration. Based on *operando* NMR kinetics, end group analysis, active site counting with chromophore quench labels, iodine quenching studies, and gel permeation chromatography, we propose a unified kinetic and mechanistic model for the polymerization of 1-octene with **2**.

KEYWORDS: *alkene polymerization, kinetics, mechanism, active site counting, dual-chain growth, dormancy*

INTRODUCTION

Polyalkenes such as polyethene, polypropene, other poly(1-alkenes), and their copolymers continue to increase in popularity for a variety of commercial and industrial applications.[1] As a result, homogeneous catalysts for alkene polymerization continue to elicit intense research interest.[2] This interest is due to homogeneous catalysts' ability to generate polymers with low dispersity (*Đ*), high molecular weight, and well-defined polymer microstructure.[3] In pursuit of catalyst discovery and improvement, a plethora of ligand architectures and metal complexes have been developed, reportedly numbering in the thousands.[4] These include catalysts containing both early and late transition metals that together are capable of producing polymers with a variety of molecular weights, *Đ*, and microstructures.[2a,3a−d,f,5] In order to provide a foundation for continuing catalyst design and improvement, careful mechanistic studies are vital to understanding the differential activity of catalyst architectures.

Our understanding of homogeneous catalysis is primarily derived from kinetic studies because catalysis is a wholly kinetic phenomenon. For polymerization catalysts, saturation behavior with respect to alkene is distinctive. Catalysts made from late transition metals commonly exhibit polymerization rates that are independent of monomer concentration.[5b,6] Such saturation behavior is induced by rapid, reversible, and favorable binding of monomer to the catalyst prior to alkene insertion (Figure 1).[5b,6a,7] On the other hand, early transition-metal catalysts usually exhibit rate laws that display first-order dependence on monomer concentration.[8]

Superficially, different orders in monomer concentration may suggest different mechanisms. However, more detailed analysis indicates similarities in the mechanism for early and late transition-metal propagation steps. While d^n late transition-

Received: March 11, 2022
Revised: July 18, 2022
Published: August 16, 2022

https://doi.org/10.1021/acscatal.2c01240
ACS Catal. 2022, 12, 10680−10689

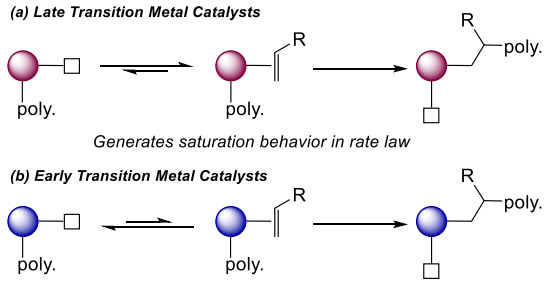

Figure 1. Proposed mechanisms for monomer insertion during polymer propagation for (a) late and (b) early transition-metal catalysts.

metal complexes bind alkenes favorably, d^0 early transition-metal centers do not.[9] Reversible binding of monomer prior to insertion at early transition-metal catalysts is supported by heavy-atom kinetic isotope effects.[10] However, because the binding is not particularly favorable, the early transition-metal catalysts do not exhibit saturation behavior. Thus, most early transition metals display rate laws with a first-order dependence on the concentration of monomer. Whether zero-order rate behavior is diagnostic of saturation kinetics, however, is an open question that we will address in this paper.

First introduced by Murray and coworkers at Union Carbide, imino-amido ligand frameworks became popular for polymerization catalysts due to ease of synthesis, production of desirable polymer characteristics, and tunability of both metals and substituents.[11] The imino-amido ligated precatalyst $(N^{oct}N^{dipp})$-$Hf(Me)_3$ ($N^{oct}N^{dipp}$ = *N*-octyl-*N*′-(2,6-diisopropylphenyl)-1,4-diaza-2,3,3-trimethyl-1-butene, **1**, Figure 2a) has been previously reported for various polymerization reactions including the copolymerization of ethylene with 1-octene.[11a] Additionally, **1** has been reported as a competent precatalyst for chain-shuttling block copolymerization of ethylene and 1-octene.[3d,11d,12]

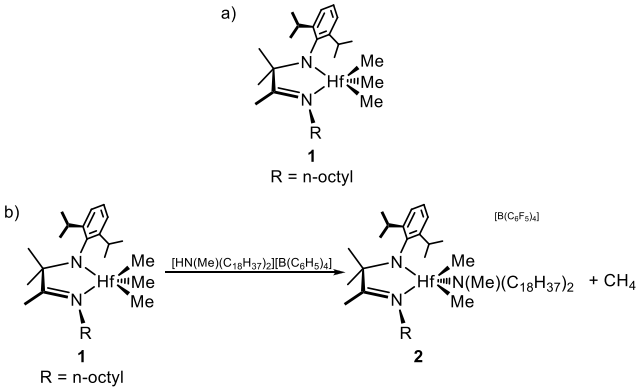

Figure 2. (a) Structure of precatalyst **1** and (b) its protonolysis to form **2**.

Importantly, **1** features a nontraditional structural feature: the presence of three Hf−Me groups. Protonolysis with the Brønsted acid $[HN(Me)(C_{18}H_{37})_2][B(C_6F_5)_4]$ forms the catalytically active, monomeric species $[(N^{oct}N^{dipp})Hf(Me)_2(N(Me)(C_{18}H_{37})_2)][B(C_6F_5)_4]$ (**2**, Figure 2b), in which the catalyst retains two Hf−Me groups. Characterization of this complex supports the assignment of **2** as a monomer based on diffusion NMR studies (see the Supporting Information). Each Hf−Me group is theoretically capable of 1,2-insertion of monomer into the Hf−C bond, resulting in a catalyst that can propagate two polymer chains on each metal center. Previous reports indicate that both methyls can undergo insertion of a diene to form a cycloalkyl hafnium complex.[13] However, no compelling evidence for growth of two polymer chains at a metal center has been reported. Additionally, knowing the concentration of actively propagating sites for polymer growth is key to the development of kinetic models with high fidelity and predictive accuracy.[14]

Details of how **2** operates in catalysis are scarce. Fundamental information that is unknown includes: (1) the fraction of **2** that is active in catalysis under different conditions; (2) the rate law for polymerization; (3) the number of propagating chains per catalyst; and (4) catalyst speciation under reaction conditions. Herein, we present the development of a quantitative, phenomenological kinetic model for the polymerization of 1-octene by **2** based on *operando* NMR monitoring of polymerization reactions, isotopic labeling studies, chromophore quench labeling, and iodinolysis quenching experiments. These techniques enable determination of active site counts, the rate law for polymerization, the number of chains growing on each catalyst, and catalyst speciation. Additionally, we present conclusive evidence that the catalyst grows two polymer chains on each hafnium center throughout the catalysis.

RESULTS AND DISCUSSION

2 Produces Polymer with Unexpected Characteristics.

Even though the catalyst is achiral, it generates isotactic polyoctene with minimal regio-errors as determined by ^{13}C NMR spectroscopy (see the Supporting Information).[15] The polymer is mostly isotactic but with approximately 26% stereo-errors.[16] Chain-end control could account for the tacticity.[16b,17] An alternative hypothesis is that the presence of a second polymer chain growing on the metal itself provides a stereocenter directly adjacent to the metal. The ^{13}C NMR of the polymer is not consistent with the presence of a significant number of enchained 2,1-insertions.[18] End-group analysis by ^1H NMR spectroscopy reveals a predominance of vinylene end groups over vinylidene end groups in an approximately 10:1 ratio under most conditions. This ratio suggests that termination from secondary alkyl species generated by a 2,1-insertion dominates. Together, these data indicate that 2,1-insertions occur, but the resultant secondary alkyls do not propagate further.

Analysis of a single timecourse of 1-octene polymerization produced by **2** reveals a number-average molecular weight (M_n) of approximately 5300 amu and $Đ$ = 1.6. Although the modal molecular weight does shift slightly during a reaction (Figure 3a), the molecular weight averages M_n and M_w do not (Figure 3b). The apparent shift in modal molecular weight is due to the non-Gaussian shape of the molecular weight distribution obtained, particularly at short reaction times. Unlike most transition-metal-catalyzed polymerizations, where M_n and M_w depend on the monomer concentration and change during a reaction, the values of M_n and M_w essentially are independent of the transient monomer concentration within a single reaction.

The molecular weight of poly(1-octene) produced by **2** exhibits slight dependence on the *initial* monomer concentration. Plots of M_n and M_w versus the average octene concentration for a set of reactions started at different initial concentrations of 1-octene (Figure 4) show small decreases of M_n and M_w as the average concentration of monomer is increased (e.g., Mn changes from ca. 5000 amu to ca. 4500 amu

https://doi.org/10.1021/acscatal.2c01240
ACS Catal. 2022, 12, 10680−10689

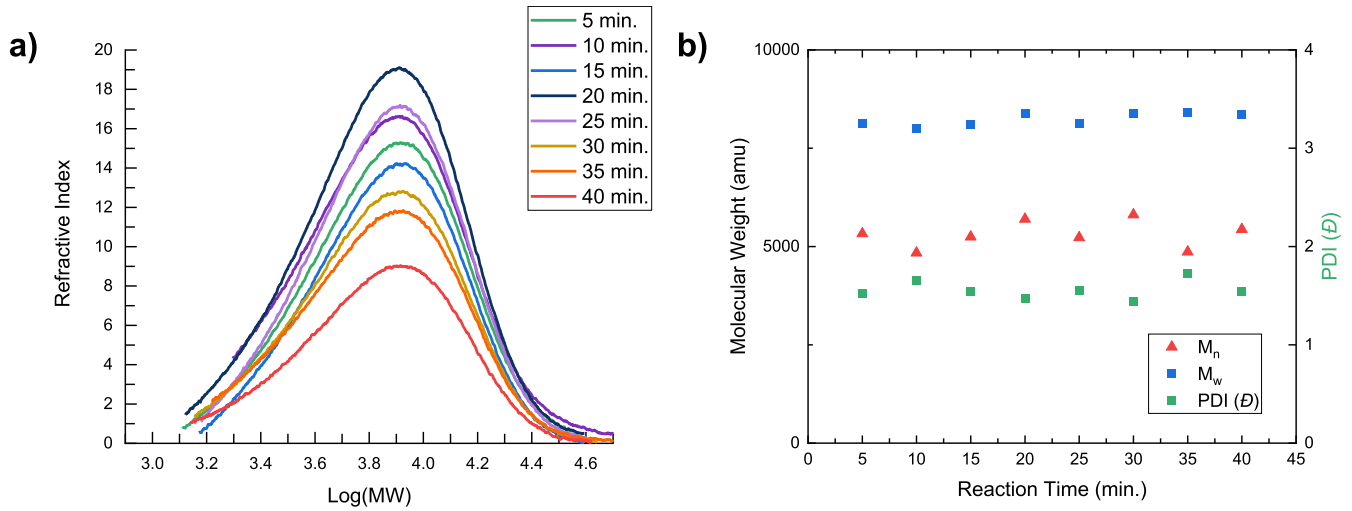

Figure 3. (a) GPC of poly(1-octene) produced in reactions quenched between 5 and 40 min. Polymerization reactions were run at 50 °C with toluene as the solvent (total volume = 1 mL); $[1\text{-octene}]_0$ = 503.2 mM; $[\mathbf{2}]_0$ = 0.0829 mM. (b) Molecular weight averages [M_n, ▲ (red triangle symbol); M_w, ■ (blue square symbol)] and polydispersity [$Đ$, ■ (green square symbol)] of polymer as determined by GPC with chromatograms in part (a).

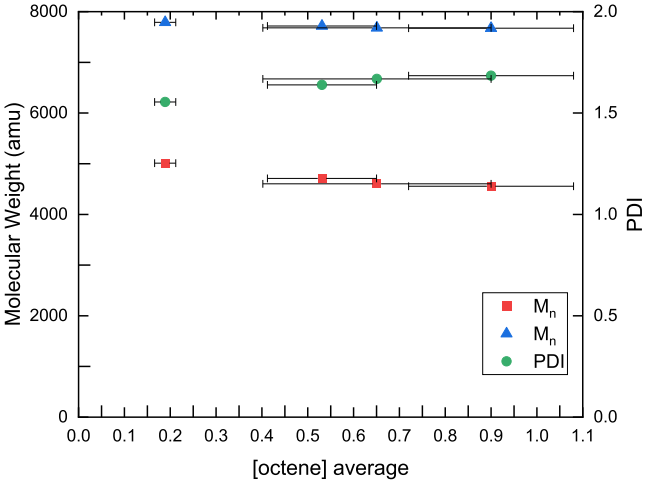

Figure 4. Dependence of molecular weight averages M_n and M_w and PDI on initial concentration of 1-octene, where bars parallel to the x-axis show the range of octene concentration during the reaction. Polymerization reactions were run at 50 °C with toluene as the solvent (total volume = 1 mL); $[1\text{-octene}]_0$ varied from 0.21 to 1.08 M; $[\mathbf{2}]_0$ = 4.01 mM.

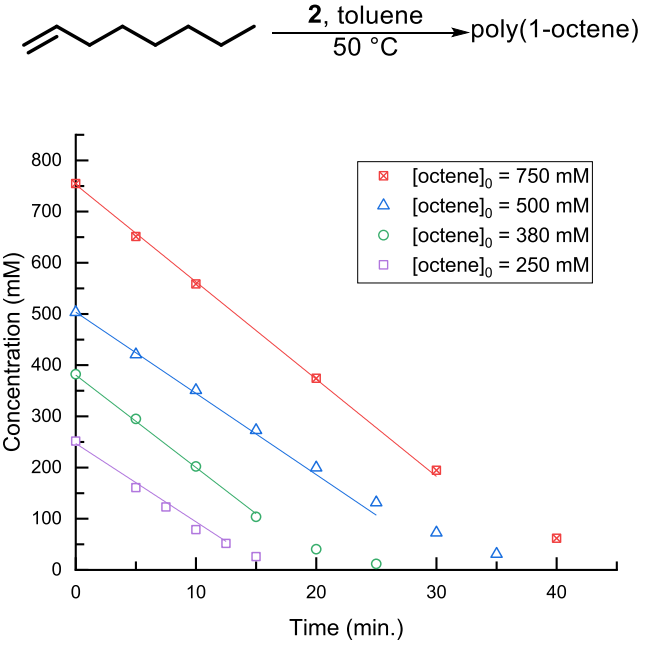

Figure 5. Timecourses of 1-octene polymerization by **2** at 380 mM [□ (violet square symbol)], 250 mM [○ (green circle symbol)], 500 mM [△ (blue diamond symbol)], and 750 mM [red square with multiplication symbol] initial concentrations of 1-octene. Polymerization reactions were run at 50 °C with toluene as the solvent (total volume = 1 mL); $[\mathbf{2}]_0$ = 0.0829 mM.

upon increasing $[\text{monomer}]_{ave}$ from 0.2 to 0.9 M). There are several plausible explanations for these data.

One plausible explanation for the effective independence of polymer molecular weight on the transient monomer concentration is termination of chain growth by chain transfer to the monomer. If chain propagation and chain transfer both are first-order in monomer, the average mass of the polymer effectively would be independent of the monomer concentration. Chain transfer to monomer could occur from either primary or secondary alkyls; the former produces vinylidene end groups, and the latter generates vinylenes. Vinylene end groups are dominant, meaning that chain termination mostly occurs from secondary alkyls. Exclusive chain termination via chain transfer to the monomer requires that the rate of appearance of vinylene (or vinylidene) end groups be first-order in monomer concentration. The observed rate of vinylene end groups' appearance is not linear with respect to the monomer concentration (Figure S40 in the Supporting Information). The rate of vinylene production asymptotically saturates at ~0.0115 mM/s with increasing [1-octene]. Furthermore, the observed rate of production of vinylidene chain ends is inverse first-order in monomer concentration. (Figure S41). These observations are inconsistent with chain transfer to the monomer as the dominant mechanism of chain transfer.

A second plausible mechanism that accounts for the predominate independence of M_n on the monomer concentration features fast propagation at primary Hf-polymeryls but no propagation from secondary alkyls; in other words, a

https://doi.org/10.1021/acscatal.2c01240
ACS Catal. 2022, 12, 10680−10689

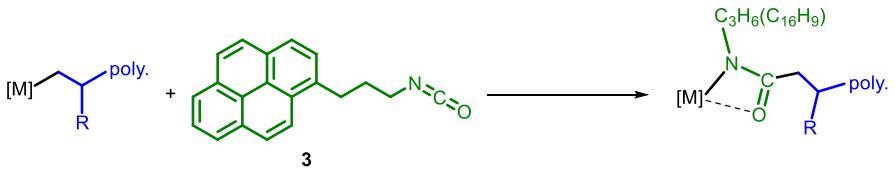

Figure 6. Generic reaction for chromophore quench labeling using pyrenyl-isocyanatopropane.

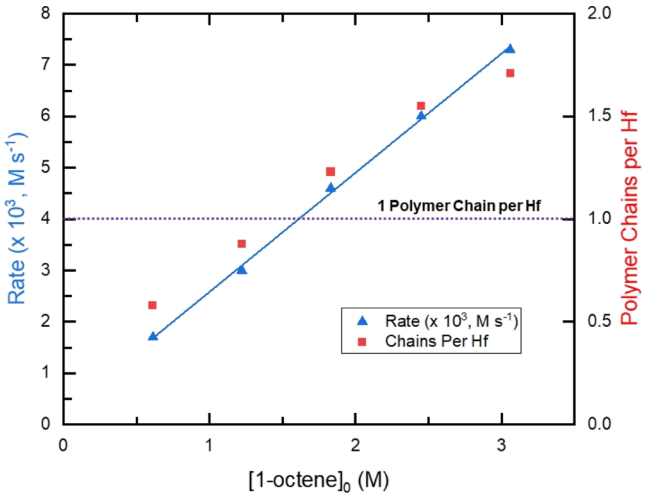

Figure 7. Dependence of observed rate of monomer consumption and active site counts from CQL on the initial monomer concentration. The best-fit line for the rate vs [octene] data has the equation rate = $0.0023[\text{octene}]_0 + 0.00026$. Polymerization reactions were run at 50 °C with toluene or toluene-d_8 as the solvent (total volume = 0.520 mL); $[\mathbf{2}]_0$ = 4.0 mM. Rates were measured by *operando* ^{1}H NMR spectroscopy and active site counts determined by quenching a reaction using **3** at 60 s.

dormant site mechanism. Detailed evidence that supports this mechanism is discussed below.

2 Exhibits Unusual Kinetic Phenomena for an Early Transition-Metal Catalyst. Observed rates of polymerization with **2** also present a surprise—despite using an early transition metal, the consumption of monomer is approximately linear over time (Figure 5). The linear consumption of monomer phenomenologically suggests that the reaction rate law is zero order in the monomer concentration. Such behavior is unusual for an early transition-metal catalyst. Counterintuitively, although the rate appears independent of the *transient* monomer concentration, the steady-state rate does appear to be dependent on the *initial* monomer concentration.

The data presented so far can be summarized as follows: (1) polymer is produced by 1,2-insertions of octene without propagation following 2,1-insertions; (2) termination after a 2,1-insertion forms a vinylene end group, which predominates over β-hydride elimination from a primary alkyl to form a vinylidene end group; (3) M_n and M_w are essentially independent of the monomer concentration; and (4) rate of monomer consumption is independent of the *transient* monomer concentration, while the steady-state rate depends on the *initial* monomer concentration.

Two Polymers Grow on the Same Metal Center. Quantitative determination of actively growing chains used the

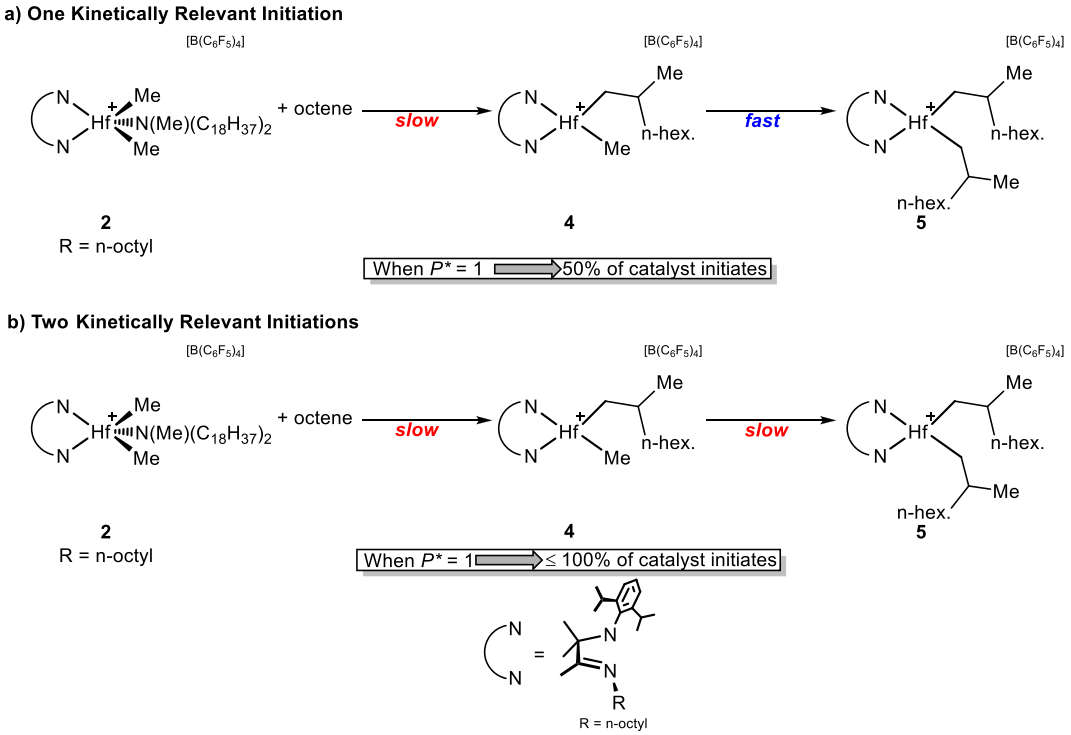

Figure 8. Possible initiation scenarios for **2** including (a) rapid initiation of a second polymer chain after the first and (b) slow initiation of a second polymer chain after the first.

https://doi.org/10.1021/acscatal.2c01240
ACS Catal. 2022, 12, 10680−10689

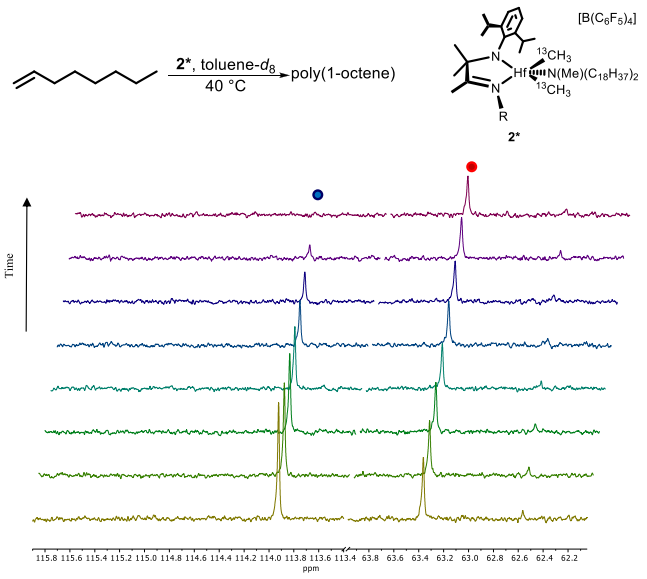

Figure 9. Monitoring of 1-octene polymerization and precatalyst initiation with **2*** by quantitative ^{13}C NMR. Reaction conditions: toluene-d_8, 40 °C, $[1\text{-octene}]_0$ = 1.45 M, $[\mathbf{2}^*]_0$ = 4.1 mM; spectra taken every 58 s. N.B.: the minor peak at 62.5 ppm is present in all samples of **2*** and is assigned as an unidentified byproduct of precatalyst activation. The upfield peak at ca. 63 ppm is assigned to the ^{13}C-enriched methyl groups of the precatalyst, while the downfield peak at ca. 114 ppm is assigned to the natural abundance 2-carbon of 1-octene.

chromophore quench label (CQL, Figure 6) 1-pyrenyl-3-isocyanatopropane (**3**).[19] Rapid injection of the CQL halts polymerization and irreversibly labels all catalyst-bound chains. Following workup with acidic methanol, the sample is analyzed by GPC. Integration of the chromophore absorption signal obtained by UV-GPC reveals the number of metal-attached polymer chains in catalysis, whereas the distribution reveals the dispersity and average molecular weight of Hf-bound polymeryls.

Using **3** (Figure 6) under the conditions noted in Figure 7, we observe the number of metal-bound polymer chains per hafnium center added to catalysis (P^*) to be dependent on the initial monomer concentration and to range from *ca.* 0.6 to *ca.* 1.7 chains per hafnium. This indicates that, under some conditions, more than one polymer chain grows at a metal center. The value of P^* appears to remain constant during the catalytic steady state.

As mentioned previously, the steady-state rate, spanning monomer concentrations 0.5−3 M, exhibits a first-order dependence on the initial monomer concentration. The steady-state value of P^* also increases with the initial concentration of monomer (Figure 7). Thus, the increase in actively growing chains with increasing initial monomer concentration accounts for the increase in the steady-state rate. These data are consistent with (1) an apparent propagation rate that is independent of monomer concentration and (2) slow catalyst initiation with a rate law that is first-order in monomer. As the initial concentration of octene increases, so does the rate of initiation, leading to an increase in P^* and more rapid monomer consumption. Similar behavior has been observed with other polymerization catalysts.[19]

Discerning Relative Rates of Initiation for the First and Second Polymer Chains. Data obtained from the CQL indicate that, under some conditions, more than one polymer chain grows on some metal centers. This is confirmed by iodinolysis, which provides an alternative method of counting actively growing polymer chains.[20] For catalysts that grow just one chain per catalyst center, P^* is equal to the proportion of catalyst that has initiated (assuming no catalyst deactivation). However, for a catalyst that is capable of propagating two polymer chains, the interpretation of P^* is more subtle. Chains counted toward P^* will include catalysts that are singly initiated and propagating one chain (**4**, Figure 8) and catalysts that are doubly initiated and propagating two chains (**5**, Figure 8, eq 1). Initiation must occur in two steps from activated $HfMe_2$: insertion into the first Hf−Me bond to initiate the first polymer chain and insertion into the second Hf−Me to grow a second chain. If the initiation of the second polymer chain is rapid relative to the initiation of the first chain, then most catalysts will grow two polymer chains (Figure 8a). If initiation of the second polymer chain is slow, however, then most of the catalysts will only grow one polymer chain (Figure 8b). For example, two limiting scenarios give rise to $P^* = 1$: (1) 50% of the catalyst (**5**) has two chains or (2) 100% of the catalyst (**4**) propagates just one chain. Any linear combination of these is possible.

$$P^* = \alpha\mathbf{4} + 2 \times \mathbf{5} \quad (1)$$

^{13}C NMR spectroscopy enables the observation and differentiation of **4**, **5**, and uninitiated catalyst. We synthesized the ^{13}C-isotopologue of **2**, **2*** to monitor catalyst initiation by ^{13}C NMR spectroscopy. Conducting a polymerization reaction at high catalyst loading (4.0 mM) and lower temperature (40 °C) allowed us to monitor precatalyst initiation by both ^{13}C and ^{1}H

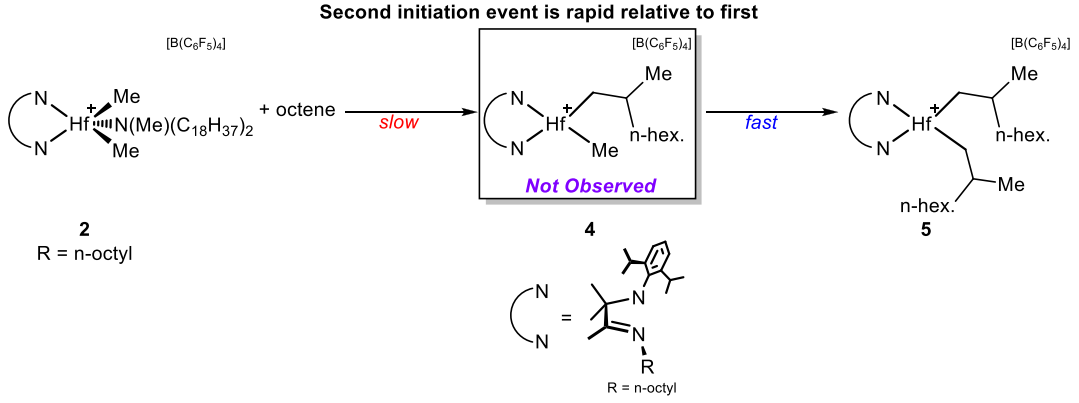

Figure 10. Proposed initiation pathway for 2.

https://doi.org/10.1021/acscatal.2c01240
ACS Catal. 2022, 12, 10680−10689

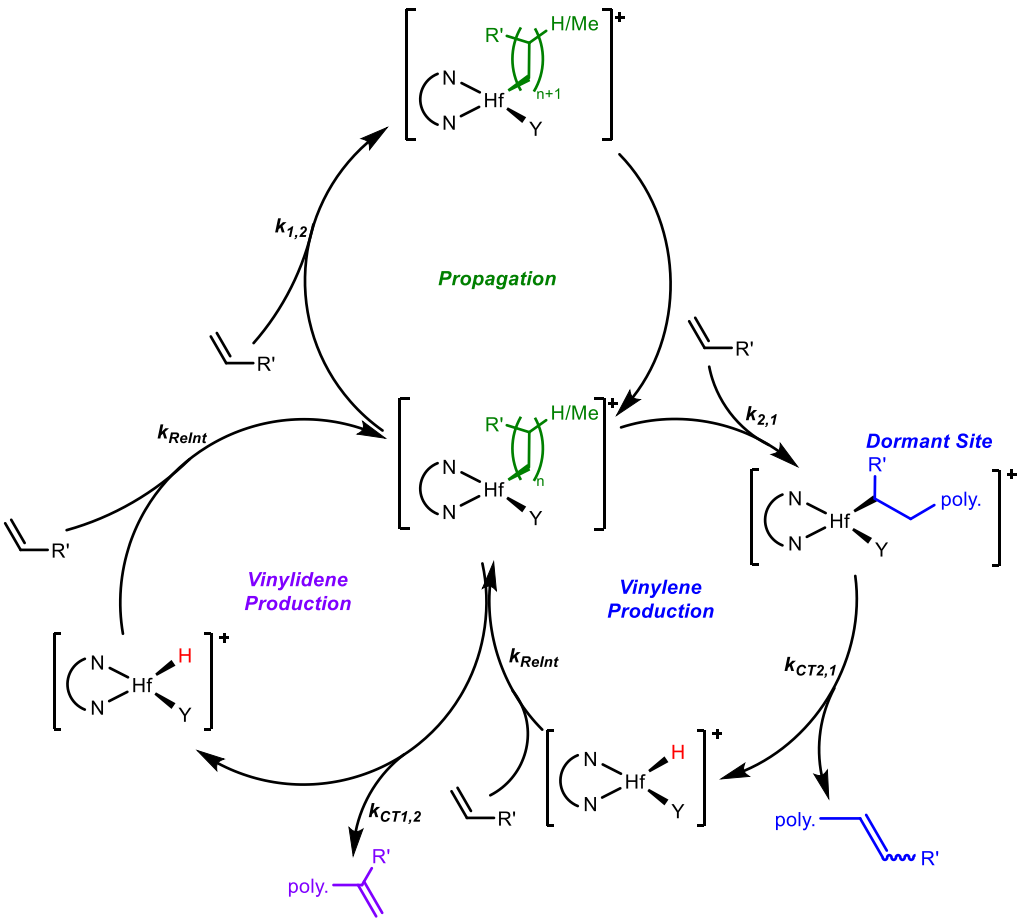

Figure 11. Qualitative mechanism for octene polymerization by **2**. Off-cycle amine-bound species are not included for clarity.

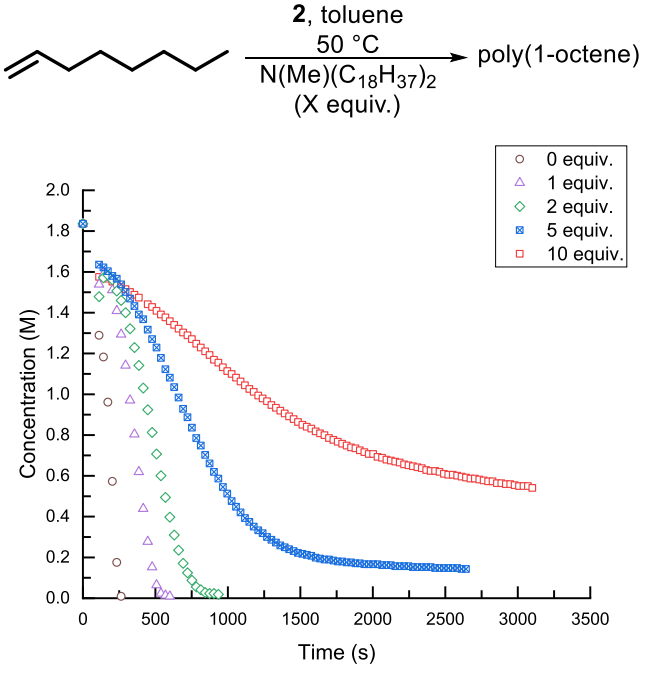

Figure 12. Timecourses obtained by *operando* ^{1}H NMR spectroscopy showing 1-octene consumption with 0−10 equiv of added N(Me)$(C_{18}H_{37})_2$ (1−11 total equiv present). Polymerization reactions were run at 50 °C with toluene-d_8 as the solvent (total volume = 0.520 mL); $[\mathbf{2}]_0$ = 4.8 mM.

NMR (Figure 9). Spectra of the reaction mixture showed only ^{13}C NMR signals assigned to 1-octene and **2***. Thus, we conclude that upon initiating the first chain, **4** reacts quickly with an additional equivalent of alkene to initiate the growth of a second polymer chain.

These data indicate that no appreciable concentration of **4** builds up during catalysis, and that either as **2** or **5** accounts for most of the catalyst.[21] This kinetic scenario requires that initiation of the second polymer chain occurs *faster* than the initiation of the first chain (Figure 10). We speculate that the origin of faster initiation of the second chain is due to amine (from activation) binding being less favorable with **4** than for **2**.

Under Catalytic Conditions, Most Metal-Bound Polymer Chains are Dormant Secondary Alkyls. Quenching catalysis with I_2 distinguishes between metal-bound primary and secondary alkyls via the ^{1}H NMR chemical shifts of the geminal proton(s) on the resultant alkyl halides.[20b] Iodinolysis reveals that, in the steady state, 95% of hafnium-bound polymer chains are secondary alkyls.

To directly observe the dormant species by ^{13}C NMR, we conducted a freeze-quench experiment. Cooling a polymerization of 1-^{13}C-1-octene to −20 °C effectively stops polymerization. The ^{13}C NMR spectrum exhibits no resonances for ^{13}C that is directly attached to Hf as expected for a primary Hf-alkyl. However, there are other observed resonances that may be consistent with secondary Hf-alkyls. A ^{13}C COSY spectrum contains multiple cross-peaks that demonstrate one-bond coupling (J_{CC} ~ 40 Hz) of two isotopically enriched carbons centers; this pattern is consistent with a 2,1-insertion occurring

https://doi.org/10.1021/acscatal.2c01240
ACS Catal. 2022, 12, 10680−10689

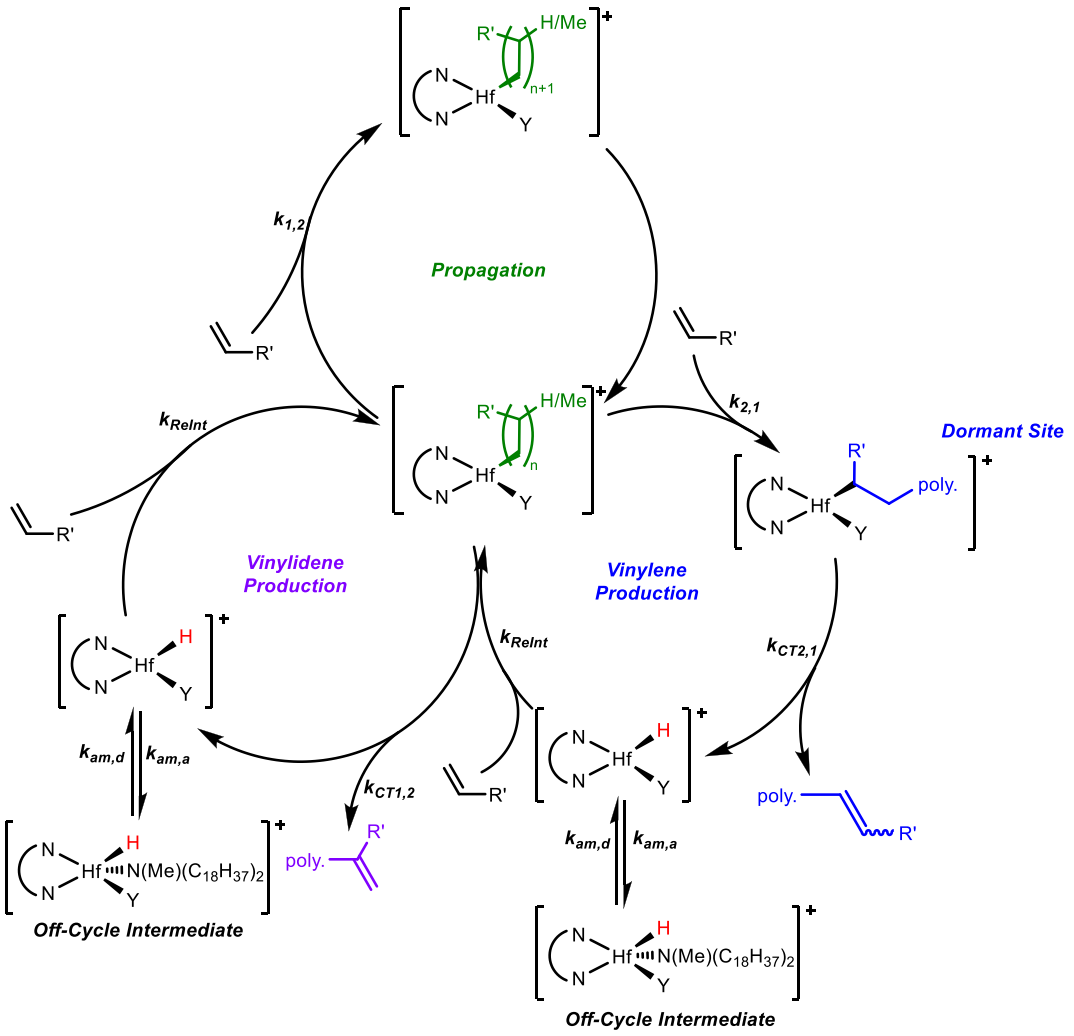

Figure 13. Mechanism with rate constants used for quantitative modeling of kinetic data for the polymerization of 1-octene by **2**.

after a 1,2-insertion. One set of cross-peaks, at chemical shifts 24.2 and 34.2 ppm, are consistent with vinylene chain ends (see the Supporting Information Table S1 for details on assignments). A second set of cross-peaks, at chemical shifts of 29.7 and 34.1 ppm, are not consistent with vinylene chain ends. The correlated resonance at 34.1 ppm shows a second one-bond C−C coupling (J_{CC} = 44.8 Hz) and a weak cross-peak with a resonance unobserved in the 1D spectrum (i.e., consistent with a low concentration, unlabeled species) at 67.2 ppm. The downfield chemical shift suggests that this peak is a Hf-bound carbon. As a result, we assign this species as a Hf-bound secondary alkyl species. Overall, the correlation spectrum is consistent with a Hf-bound secondary alkyl species being the only metal-bound species observed in the freeze-quench experiment (see the Supporting Information for more details).

The observed secondary alkyls do not undergo a subsequent 1,2-insertion as evidenced by the fact that the polymer produced by this catalyst does not have any enchained regio-errors. As a result, the resting state of the catalyst (accounting for about 95% of the catalyst) is not propagating and could be considered dormant (*vide infra*). The data indicate the following: (1) catalysts with two primary polymeryls can undergo insertion at either polymeryl; (2) catalysts with one primary polymeryl and one secondary polymeryl can undergo insertion at the primary chain only; and (3) catalysts with two secondary polymeryls cannot undergo insertion at either chain. For scenario 2, it is important to note that if the primary polymeryl could not undergo insertion, the maximum number of secondary polymeryl chains for a catalyst growing two chains simultaneously must be 50%. The maximum would be 50% because the primary chain could not undergo a 2,1-insertion to become a secondary chain, limiting each catalyst to having just one secondary chain and one primary chain. Because the primary chain must be able to undergo a 2,1-insertion, the site can likely undergo a 1,2-insertion as well, allowing propagation to take place. Because scenarios 1 and 2 grow polymers, polymer growth is independent of whether the other chain is a secondary polymeryl or not.

The existence of dormant sites has often been proposed in the alkene polymerization literature.[14,22] The critical attribute characterizing dormant sites is a temporary reduction of propagation activity. Deactivated or dead catalytic sites also have reduced propagation activity, but the reduction is permanent. In particular, M−allyls and M−2° alkyls have been proposed as dormant sites.

Qualitative Mechanistic Model. A qualitative model comprising three processes—propagation, chain transfer from primary polymeryls to form vinylidene end groups, and chain transfer from secondary polymeryls to form vinylene end groups—accommodates the data above (Figure 11). Figure 11

https://doi.org/10.1021/acscatal.2c01240
ACS Catal. 2022, 12, 10680−10689

does not show initiation events. As described above, precatalyst initiation occurs slowly relative to propagation. However, once an initiation event has occurred at one Hf−Me, initiation at the second Hf−Me is rapid. This forms a catalyst with two propagating chains as shown in Figure 10. Chain transfer from a primary polymeryl creates at vinylidene end group and hafnium hydride. Otherwise, each chain propagates until it undergoes a 2,1-insertion and becomes dormant. At the steady state, most of the hafnium-bound polymeryls exist as dormant (secondary) sites. Upon β-hydride elimination, secondary polymeryls form a vinylene chain end and a hafnium hydride. The resultant hydride reinitiates via a rapid 1,2-insertion of monomer (relative to insertion into a Hf−C bond), as is common for transition metal hydrides.[23]

$$\text{Rate of monomer consumption} = \frac{k_{1,2}[\text{Cat}]_{\text{total}}[\text{alkene}]}{1 + \frac{k_{2,1}[\text{alkene}]}{k_{\text{CT2,1}}} + \frac{k_{\text{CT1,2}} + k_{2,1}[\text{alkene}]}{k_{\text{reInit}}[\text{alkene}]}} \quad (2)$$

Application of the steady-state approximation to all catalyst species yields the rate law shown in eq 2. The concentrations of all catalyst species are collected in the $[\text{Cat}]_{\text{total}}$ term. The steady-state approximation assumes the following: (1) all catalysts initiate quickly and do not deactivate during catalysis; (2) all catalysts exist as either a hydride, primary alkyl, or secondary alkyl species; (3) after initiation, the two chains propagate *independently*; (4) after undergoing a 2,1-insertion, propagation ceases; (5) reinitiation of chain growth from the hydride is rapid relative to all other steps; and (6) amine binding effects are neglected.

Importantly, eq 2 reveals the conditions under which the steady-state rate of monomer consumption will become independent of the monomer concentration. If $\left(k_{2,1}[\text{alkene}] \gg \left(1 + \frac{k_{\text{CT1,2}} + k_{2,1}[\text{alkene}]}{k_{\text{reInit}}[\text{alkene}]}\right)k_{\text{CT2,1}}\right)$, then the rate of monomer consumption is approximately independent of the concentration of monomer. In chemical terms, this condition is satisfied when the rate of β-hydride elimination following a 2,1-insertion (determined by $k_{\text{CT2,1}}$) is much slower than the rate of a 2,1-insertion (given by $k_{2,1}[\text{alkene}]$). Necessarily, the occurrence of a rate law for propagation that is independent of the monomer concentration coincides with accumulation of the catalyst as a secondary alkyl.

Quantitative Kinetic Modeling without considering Off-Cycle Species. We examined the robustness of the qualitative model to quantitative scrutiny. Using the kinetics modeling software package Copasi,[24] we built a model of 1-octene polymerization based on Figure 11. This allows us to examine the performance of this model by quantitatively assessing the fit.

For this kinetic model, the flux of monomer consumption is accounted for by the growth of a single chain at each center. This simplification avoids accounting for the many different species that exist if two chains are growing at a metal center. Because the evidence suggests that polymer chains grow independently, the kinetic approximation of single chain growth is reasonable. As a result, each catalyst molecule in this model only grows one polymer chain.

The quantitative Copasi model for polymerization includes the reaction steps in Figure 11 and precatalyst initiation (see the Supporting Information for a list of all rate constants and reaction steps). Molecular weight distributions were modeled by fitting the values of M_n and M_w by adjustment of rate constant values. The model accurately reproduces important kinetic behavior of the system including: (1) a rate of monomer consumption at the steady state that is independent of transient monomer consumption; (2) slow initiation of the precatalyst; (3) a steady-state rate of monomer consumption that is dependent on the initial concentration of monomer; and (4) the values of M_n and M_w for the polymer produced.

$$\frac{k_{1,2}}{k_{2,1}} = \frac{M_n}{M_{w_{\text{octene}}}} = 42 \quad (3)$$

Although the data are fit well, least-squares fitting of the data leads to substantial correlation between rate constants due to the large number of parameters. To reduce parameter correlation, we fixed the ratio of $k_{1,2}/k_{2,1}$ according to the average number of monomer insertions. The average number of insertions is given in eq 3 and gives a value of 42.[25] As a result, the value of k_{21} was assigned the value of $k_{1,2}/42$. Significantly, while global fitting of all data could not be achieved, our qualitative model of polymerization can fit all data at a single catalyst concentration with a single set of rate constants.

Quantitative Kinetic Modeling: Accounting for Amine Binding. Substantially different initial concentrations of catalyst could not be modeled using the methods described above. Over catalyst concentration spanning 3 orders of magnitude, the apparent rate of the reaction is not first-order in catalyst concentration (see the Supporting Information). This suggests that an equilibrium affecting catalyst initiation and/or propagation exists. We hypothesize that free amine produced by activation of **1** (Figure 2) can reversibly bind catalyst species and inhibit catalysis.[20b] Consistent with this hypothesis, addition of excess amine $N(Me)(C_{18}H_{37})_2$ causes a significant inhibition of catalysis (Figure 12). At 10 equiv of amine, catalysis stalls prior to reaction completion.

Fitting all available kinetic data with a single set of rate constants requires modeling amine binding. The amine-bound activated species **2** can be observed directly by NMR via the distinctive Hf−Me resonances under both catalytic and non-catalytic conditions. By monitoring the disappearance of **2**, the effects of amine binding on initiation can be interrogated directly. However, the actively propagating species lack distinctive NMR markers and cannot be monitored directly. Therefore, we cannot directly interrogate the binding of amine to propagating species. Given the likelihood of binding multiple species, we modeled the effects of amine binding on propagation via the inclusion of a single equilibrium binding event that moves an on-cycle species to an off-cycle intermediate species. Which species the amine binds to in the model is unimportant; we arbitrarily chose to represent this binding via the Hf−H produced from chain-transfer events.[26]

Using a model that includes amine inhibition of both initiation and propagation (Figure 13), we can reproduce monomer consumption, the formation of vinylene and vinylidene end groups, precatalyst concentrations/active site counts, and the values of M_n and M_w with a single set of rate parameters over all conditions. The rate constants obtained from this modeling are given in the Supporting Information.[27] Because the model accurately describes all kinetic data, it is a sufficient, but not necessarily unique, model for the homopolymerization of 1-octene using **2**.

https://doi.org/10.1021/acscatal.2c01240
ACS Catal. 2022, 12, 10680−10689

CONCLUSIONS

In this paper, we have used chromophore quench labeling, I_2 quenching, *operando* ^1H and ^{13}C NMR spectroscopy, and isotopic labeling experiments to study alkene polymerization as catalyzed by **2**. This catalyst clearly illustrates the kinetic effects and polymer characteristics that result from occasional 2,1-insertions to create non-propagating (dormant) secondary alkyl sites. Thus, **2** constitutes an *authentic* example of the oft-proposed formation of dormant sites in catalytic alkene polymerization.

Catalyst **2** exhibits the following characteristics: (1) M_n and M_w are independent of the monomer concentration; (2) a predominance of vinylene end groups over vinylidene end groups; (3) an active catalyst primarily residing as a secondary alkyl; (4) the growth of two polymer chains at each metal center; (5) zeroth-order dependence of the steady-state rate on the monomer concentration as a result of accumulation of catalyst in the form of dormant secondary alkyls; (6) dependence of steady-state rate on the *initial* monomer concentration due to increased catalyst initiation. Taken together, the data and analysis of **2** conclusively demonstrate that rate laws that are zeroth-order in the monomer do not require saturation of the alkene binding pre-equilibrium. The characteristics described above are diagnostic for the identification of catalysts that exist primarily as dormant secondary alkyl sites.

ASSOCIATED CONTENT

Supporting Information

The Supporting Information is available free of charge at https://pubs.acs.org/doi/10.1021/acscatal.2c01240.

General experimental considerations, methods for measuring kinetics of polymerization by NMR and quenching kinetics, methods for iodine quench labeling, freeze-quenching of polymerization, derivation of rate law for monomer consumption using steady-state approximation, COPASI modeling, and NMR spectra (PDF)

AUTHOR INFORMATION

Corresponding Author

Clark R. Landis − *The Department of Chemistry, University of Wisconsin−Madison, 1101 University Avenue, Madison, Wisconsin 53706, United States;* orcid.org/0000-0002-1499-4697; Email: landis@chem.wisc.edu

Authors

Tanner McDaniel − *The Department of Chemistry, University of Wisconsin−Madison, 1101 University Avenue, Madison, Wisconsin 53706, United States*

Nicholas E. Smith − *The Department of Chemistry, University of Wisconsin−Madison, 1101 University Avenue, Madison, Wisconsin 53706, United States*

Eric Cueny − *The Department of Chemistry, University of Wisconsin−Madison, 1101 University Avenue, Madison, Wisconsin 53706, United States;* orcid.org/0000-0003-1244-2407

Complete contact information is available at: https://pubs.acs.org/10.1021/acscatal.2c01240

Author Contributions

†T.M. and N.E.S. contributed equally.

Notes

The authors declare no competing financial interest.

ACKNOWLEDGMENTS

This work was supported by The Dow Chemical Company. We thank Dr. Heather Spinney and Dr. Robert D. J. Froese for helpful discussions. We acknowledge the Paul and Margaret Bender Fund along with the NSF (CHE-1048642 and CHE-2017891) and NIH (S10 OD012245) for the support of the NMR facility. We thank Dr. Anna Kiyanova from the UW-Madison Soft Materials Characterization Laboratory (SMCL) for assistance with GPC instrumentation and acknowledge funding of the SMCL from the NSF via the University of Wisconsin Nanoscale Science and Engineering Center (DMR-0832760 and 0425880).

REFERENCES

(1) (a) Sita, L. R. Ex Uno Plures ("Out of One, Many"): New Paradigms for Expanding the Range of Polyolefins through Reversible Group Transfers. *Angew. Chem., Int. Ed.* **2009**, *48*, 2464−2472. (b) Busico, V. Metal-catalysed olefin polymerisation into the new millennium: a perspective outlook. *Dalton Trans.* **2009**, 8794−8802.

(2) (a) Stürzel, M.; Mihan, S.; Mülhaupt, R. From Multisite Polymerization Catalysis to Sustainable Materials and All-Polyolefin Composites. *Chem. Rev.* **2016**, *116*, 1398−1433. (b) Collins, R. A.; Russell, A. F.; Mountford, P. Group 4 metal complexes for homogeneous olefin polymerisation: a short tutorial review. *Appl. Petrochem. Res.* **2015**, *5*, 153−171.

(3) (a) Baier, M. C.; Zuideveld, M. A.; Mecking, S. Post-Metallocenes in the Industrial Production of Polyolefins. *Angew. Chem., Int. Ed.* **2014**, *53*, 9722−9744. (b) Braunschweig, H.; Breitling, F. M. Constrained geometry complexes—Synthesis and applications. *Coord. Chem. Rev.* **2006**, *250*, 2691−2720. (c) Makio, H.; Terao, H.; Iwashita, A.; Fujita, T. FI Catalysts for Olefin Polymerization-A Comprehensive Treatment. *Chem. Rev.* **2011**, *111*, 2363−2449. (d) Yuan, S.-F.; Yan, Y.; Solan, G. A.; Ma, Y.; Sun, W.-H. Recent advancements in N-ligated group 4 molecular catalysts for the (co)polymerization of ethylene. *Coord. Chem. Rev.* **2020**, *411*, 213254. (e) Brintzinger, H. H.; Fischer, D.; Mülhaupt, R.; Rieger, B.; Waymouth, R. M. Stereospecific Olefin Polymerization with Chiral Metallocene Catalysts. *Angew. Chem., Int. Ed.* **1995**, *34*, 1143−1170. (f) Britovsek, G. J. P.; Gibson, V. C.; Wass, D. F. The Search for New-Generation Olefin Polymerization Catalysts: Life beyond Metallocenes. *Angew. Chem., Int. Ed.* **1999**, *38*, 428−447.

(4) Chen, C. Designing catalysts for olefin polymerization and copolymerization: beyond electronic and steric tuning. *Nat. Rev. Chem.* **2018**, *2*, 6−14.

(5) (a) Gibson, V. C.; Spitzmesser, S. K. Advances in Non-Metallocene Olefin Polymerization Catalysis. *Chem. Rev.* **2003**, *103*, 283−316. (b) Ittel, S. D.; Johnson, L. K.; Brookhart, M. Late-Metal Catalysts for Ethylene Homo- and Copolymerization. *Chem. Rev.* **2000**, *100*, 1169−1204.

(6) (a) Gates, D. P.; Svejda, S. A.; Oñate, E.; Killian, C. M.; Johnson, L. K.; White, P. S.; Brookhart, M. Synthesis of Branched Polyethylene Using (α-Diimine)nickel(II) Catalysts: Influence of Temperature, Ethylene Pressure, and Ligand Structure on Polymer Properties. *Macromolecules* **2000**, *33*, 2320−2334. (b) Lanni, E. L.; McNeil, A. J. Mechanistic Studies on Ni(dppe)Cl_2-Catalyzed Chain-Growth Polymerizations: Evidence for Rate-Determining Reductive Elimination. *J. Am. Chem. Soc.* **2009**, *131*, 16573−16579.

(7) (a) Johnson, L. K.; Killian, C. M.; Brookhart, M. New Pd(II)- and Ni(II)-Based Catalysts for Polymerization of Ethylene and α-Olefins. *J. Am. Chem. Soc.* **1995**, *117*, 6414−6415. (b) Tempel, D. J.; Brookhart, M. The Dynamics of the β-Agostic Isopropyl Complex (ArNC(R)−C(R)NAr)Pd(CH(CH_2-μ-H)(CH_3))$^+BAr_4^-$ (Ar = 2,6-C_6H_3(i-Pr)$_2$): Evidence for In-Place Rotation versus Dissociation of the Agostic Methyl Group. *Organometallics* **1998**, *17*, 2290−2296.

(8) Although rare, early transition metal complexes have been previously reported to exhibit rate laws for polymerization which is zeroth order in monomer. For example, the FI catalyst bis[*N*-(3-*tert*-butylsalicylidene)anilinato]titanium(IV) dichloride activated with

triisobutylaluminum and $Ph_3CB(C_6F_5)_4$ demonstrates a rate of polymerization of 1-hexene independent of the initial concentration of monomer, although no cause for the behavior was definitively determined. See Saito, J.; Suzuki, Y.; Makio, H.; Tanaka, H.; Onda, M.; Fujita, T. Polymerization of Higher α-Olefins with a Bis(Phenoxyimine)Ti Complex/*i*-$Bu_3Al/Ph_3CB(C_6F_5)_4$: Formation of Stereo- and Regioirregular High Molecular Weight Polymers with High Efficiency. *Macromolecules* **2006**, *39*, 4023−4031.

(9) Crabtree, R. H. *The Organometallic Chemistry of the Transition Metals*; Wiley, 2014; pp 134−162.

(10) Landis, C. R.; Rosaaen, K. A.; Uddin, J. Heavy-Atom Kinetic Isotope Effects, Cocatalysts, and the Propagation Transition State for Polymerization of 1-Hexene Using the *rac*-$(C_2H_4(1\text{-indenyl})_2)ZrMe_2$ Catalyst Precursor. *J. Am. Chem. Soc.* **2002**, *124*, 12062−12063.

(11) (a) De Waele, P.; Jazdzewski, B. A.; Klosin, J.; Murray, R. E.; Theriault, C. N.; Vosejpka, P. C.; Petersen, J. L. Synthesis of Hafnium and Zirconium Imino−Amido Complexes from Bis-imine Ligands. A New Family of Olefin Polymerization Catalysts. *Organometallics* **2007**, *26*, 3896−3899. (b) Murray, R. E. Catalyst for the production of olefin polymers. WO 1999001481 A2, 1999. (c) Murray, R. E. Imino-amide catalyst compositions for the polymerization of olefins. WO 2003051935 A1, 2003. (d) Klosin, J.; Fontaine, P. P.; Figueroa, R. Development of Group IV Molecular Catalysts for High Temperature Ethylene-α-Olefin Copolymerization Reactions. *Acc. Chem. Res.* **2015**, *48*, 2004−2016.

(12) Kuhlman, R. L.; Klosin, J. Tuning Block Compositions of Polyethylene Multi-Block Copolymers by Catalyst Selection. *Macromolecules* **2010**, *43*, 7903−7904.

(13) Sun, L.; Szuromi, E.; Karjala, T.; Zhou, Z.; Carnahan, E. Synthesis of Chain Shuttling Organometallic Compounds Capable of Producing Triblock Polyolefins. *Macromolecules* **2020**, *53*, 10796−10802.

(14) Desert, X.; Carpentier, J.-F.; Kirillov, E. Quantification of active sites in single-site group 4 metal olefin polymerization catalysis. *Coord. Chem. Rev.* **2019**, *386*, 50−68.

(15) Although the polyoctene produced is isotactic, it is important to note that this may not hold for the polymerization of other monomers.

(16) (a) Galland, G. B.; Da Silva, L. F.; Nicolini, A. Tacticity of poly-α-olefins from poly-1-hexene to poly-1-octadecene. *J. Polym. Sci., Part A: Polym. Chem.* **2005**, *43*, 4744−4753. (b) Resconi, L.; Cavallo, L.; Fait, A.; Piemontesi, F. Selectivity in Propene Polymerization with Metallocene Catalysts. *Chem. Rev.* **2000**, *100*, 1253−1346.

(17) Coates, G. W. Precise Control of Polyolefin Stereochemistry Using Single-Site Metal Catalysts. *Chem. Rev.* **2000**, *100*, 1223−1252.

(18) Landis, C. R.; Christianson, M. D. Metallocene-catalyzed alkene polymerization and the observation of Zr-allyls. *Proc. Natl. Acad. Sci. U.S.A.* **2006**, *103*, 15349−15354.

(19) Nelsen, D. L.; Anding, B. J.; Sawicki, J. L.; Christianson, M. D.; Arriola, D. J.; Landis, C. R. Chromophore Quench-Labeling: An Approach to Quantifying Catalyst Speciation As Demonstrated for $(EBI)ZrMe_2/B(C_6F_5)_3$-Catalyzed Polymerization of 1-Hexene. *ACS Catal.* **2016**, *6*, 7398−7408.

(20) (a) The use of I_2 as a quenching reagent, similar to the use of a CQL, stops the reaction and places a chemical tag, in this case an alkyl halide, on metal-bound polymer chains. This allows for total quantification of metal-bound polymer chains. Using ^1H NMR, the geminal protons for the 1° and 2° alkyl halides produced from 1° and 2° polymer chains can be independently quantified. Discussion of the findings in re catalyst speciation are discussed later in the manuscript. (b) Cueny, E. S.; Landis, C. R. The Hafnium-Pyridyl Amido-Catalyzed Copolymerization of Ethene and 1-Octene: How Small Amounts of Ethene Impact Catalysis. *ACS Catal.* **2019**, *9*, 3338−3348. (c) Cueny, E. S.; Sita, L. R.; Landis, C. R. Quantitative Validation of the Living Coordinative Chain-Transfer Polymerization of 1-Hexene Using Chromophore Quench Labeling. *Macromolecules* **2020**, *53*, 5816−5825. (d) Wallace, M. A.; Burkey, A. A.; Sita, L. R. Phenyl-Terminated Polyolefins via Living Coordinative Chain Transfer Polymerization with $ZnPh_2$ as a Chain Transfer Agent. *ACS Catal.* **2021**, *11*, 10170−10178.

(21) This experiment is limited by the relatively high limit of detection in an NMR experiment. Therefore, we can only state with certainty that **4** does not build up to account for > ∼5% of the catalyst speciation at any point in the reaction. Because **4** must exist as an intermediate even in concurrent initiation, but it does not build up, the overwhelming majority of initiated catalyst must be propagating two polymer chains.

(22) (a) Yu, Y.; Busico, V.; Budzelaar, P. H. M.; Vittoria, A.; Cipullo, R. Of Poisons and Antidotes in Polypropylene Catalysis. *Angew. Chem., Int. Ed.* **2016**, *55*, 8590−8594. (b) Busico, V.; Cipullo, R.; Romanelli, V.; Ronca, S.; Togrou, M. Reactivity of Secondary Metal−Alkyls in Catalytic Propene Polymerization: How Dormant Are "Dormant Chains". *J. Am. Chem. Soc.* **2005**, *127*, 1608−1609. (c) Desert, X.; Proutiere, F.; Welle, A.; Den Dauw, K.; Vantomme, A.; Miserque, O.; Brusson, J.-M.; Carpentier, J.-F.; Kirillov, E. Zirconocene-Catalyzed Polymerization of α-Olefins: When Intrinsic Higher Activity Is Flawed by Rapid Deactivation. *Organometallics* **2019**, *38*, 2664−2673. (d) Novstrup, K. A.; Travia, N. E.; Medvedev, G. A.; Stanciu, C.; Switzer, J. M.; Thomson, K. T.; Delgass, W. N.; Abu-Omar, M. M.; Caruthers, J. M. Mechanistic Detail Revealed via Comprehensive Kinetic Modeling of $[rac\text{-}C_2H_4(1\text{-indenyl})_2ZrMe_2]$-Catalyzed 1-Hexene Polymerization. *J. Am. Chem. Soc.* **2010**, *132*, 558−566.

(23) Crabtree, R. H. *The Organometallic Chemistry of the Transition Metals*; Wiley, 2014; pp 185−203.

(24) Hoops, S.; Sahle, S.; Gauges, R.; Lee, C.; Pahle, J.; Simus, N.; Singhal, M.; Xu, L.; Mendes, P.; Kummer, U. COPASI—a complex pathway simulator. *Bioinformatics* **2006**, *22*, 3067−3074.

(25) Hiemenz, P. C. L.; Timothy, P. *Polymer Chemistry*; CRC Press: Boca Raton, FL, USA, 2007; pp 77−115.

(26) Brezny, A. C.; Landis, C. R. Development of a Comprehensive Microkinetic Model for Rh(bis(diazaphospholane))-Catalyzed Hydroformylation. *ACS Catal.* **2019**, *9*, 2501−2513.

(27) Values of the rate constants obtained from our kinetic modeling, as well as comparisons of experimental kinetic data with simulated timecourses under corresponding conditions are given in the Supporting Information. Because we cannot confirm the exact speciation of amine binding, and due to correlation between rate constants, we cannot conclusively determine a specific set of unique, elementary rate constants for this system. However, because all data was able to be fit using a single set of parameters, our picture of polymerization with this system withstands the limits of our quantitative assessments.

https://doi.org/10.1021/acscatal.2c01240
ACS Catal. 2022, 12, 10680−10689